Т. 88, № 2 **ЖУРНАЛ ПРИКЛАДНОЙ СПЕКТРОСКОПИИ** МАРТ — АПРЕЛЬ 2021

V. 88, N 2 **JOURNAL OF APPLIED SPECTROSCOPY** MARCH — APRIL 2021

NOVEL TRIDENTATE BISOXIME CHEMOSENSOR FOR SELECTIVE RECOGNITION OF Cu^{2+} AND Zn^{2+} WITH DIFFERENT MECHANISMS [**]

W.-T. Guo [1], Y.-D. Peng [1,2], Y. Zhang [1], H. Zhang [2], Y.-L. Jiang [3*]

[1] School of Chemical and Biological Engineering at Lanzhou Jiaotong University,
Lanzhou, Gansu, 730070, China
[2] Department of Energy Engineering, Wuwei Occupational College,
Wuwei 733000, China
[3] School of Chemical Engineering and Energy at Zhengzhou University,
Zhengzhou 45000l, Henan, China; e-mail: jyl@zzu.edu.cn

A novel tridentate bisoxime chemosensor HL has been developed as a two-in-one platform for colorimetric recognition of Cu^{2+} (from blue to green), and fluorescent recognition of Cu^{2+} (fluorescence quenching) and Zn^{2+} (fluorescence enhancement) in aqueous solution (CH_3OH/H_2O, 9:1, v/v). The UV-Vis and fluorescent spectra, IR, NMR, and density functional theory (DFT) calculations indicate that the recognition mechanism for quenching the fluorescence of the HL sensor for Cu^{2+} is a photoinduced electron transfer process (PET) between the recognition group (phenolic hydroxyl group and Schiff-base group) of the sensor and the signal reporter group (benzene ring), and the enhanced fluorescence recognition mechanism of the HL sensor for Zn^{2+} is of its hindered PET process.

Keywords: *molecule sensor, colorimetric recognition, UV visible recognition, fluorescence recognition, Cu^{2+} and Zn^{2+} ions, density functional theoty calculation.*

ТРИДЕНТАТНЫЙ БИСОКСИМОВЫЙ ХЕМОСЕНСОР ДЛЯ СЕЛЕКТИВНОГО РАСПОЗНАВАНИЯ Cu^{2+} и Zn^{2+} С ИСПОЛЬЗОВАНИЕМ РАЗЛИЧНЫХ МЕХАНИЗМОВ

W.-T. Guo [1], Y.-D. Peng [1,2], Y. Zhang [1], H. Zhang [2], Y.-L. Jiang [3*]

УДК 543.43;535.37

[1] Школа химической и биологической инженерии Университета Ланьчжоу Цзяотон,
Ланьчжоу, Ганьсу, 730070, Китай
[2] Отдел энергетического машиностроения, Увэйский профессиональный колледж,
Увэй 733000, Китай
[3] Школа химической инженерии и энергетики Университета Чжэнчжоу,
Чжэнчжоу 45000l, Хэнань, Китай; e-mail: jyl@zzu.edu.cn

(Поступила 4 февраля 2020)

Разработан тридентатный бисоксимовый хемосенсор HL в виде платформы "два в одном" для колориметрического распознавания Cu^{2+} (от синего до зеленого) и флуоресцентного распознавания Cu^{2+} (тушение флуоресценции) и Zn^{2+} (усиление флуоресценции) в водном растворе (CH_3OH/H_2O, 9:1). Спектры поглощения в УФ-видимой области, а также спектры флуоресценции, ИК, ЯМР и расчеты методом теории функционала плотности показывают, что механизмом распознавания Cu^{2+} по тушению флуоресценции сенсора HL является фотоиндуцированный перенос электронов (ФПЭ) между группой распознавания (фенольная гидроксильная группа и группа основания Шиффа) сенсора и сигнальной группой (бензольное кольцо), а распознавание Zn^{2+} по усиленной флуоресценции сенсора HL основано на заторможенном процессе ФПЭ.

Ключевые слова: *молекулярный датчик, колориметрическое распознавание, распознавание по спектрам в УФ-видимой области, флуоресцентное распознавание, ионы Cu^{2+} и Zn^{2+}, расчеты методом теории функционала плотности.*

[**] Full text is published in JAS V. 88, No. 2 (http://springer.com/journal/10812) and in electronic version of ZhPS V. 88, No. 2 (http://www.elibrary.ru/title_about.asp?id=7318; sales@elibrary.ru).

Introduction. Selective binding of chemical species upon molecular recognition can lead to large perturbations in the host environment, particularly when the guest is ionic [1, 2], and many perturbations can be converted into a fluorescent change, or more directly, a colorimetric change that can be seen by the naked eye [3]. Due to the important role of metal ions in medicine, living systems, and the environment, many fluorescent and colorimetric chemical sensors of metal ions have been developed in recent years [4–11].

Among the metal ions, Cu^{2+} and Zn^{2+} are important targets because of their adverse health effects outside of normal physiological range [2]. Scientific studies have found that excess copper in the human body can cause cirrhosis, diarrhea, vomiting, dyskinesia, and sensory neurological disorders [12–15], and that people with zinc deficiency grow slowly and their immunity decreases, making them more susceptible to high blood pressure, heart disease, optic nerve diseases, and so on [16–18].

As a fluorescence and colorimetric sensor for metal ions, Salamo-like bisoxime ligands (Ar-CH=NO-$(CH_2)_2$-ON=CH-Ar′) have attracted widespread research interest. Due to the presence of heteroatoms, the luminescence of this Schiff base ligand comes mainly from photoinduced electron transfer (PET) [19]. Complexes formed by Cu^{2+} and ligands with an electron-donating atom such as oxygen or nitrogen, especially Schiff base ligands, have the highest stability constants [20, 21].

In 2015, Mergu et al. [22] designed a novel colorimetric detection probe for Cu^{2+} based on a Schiff base ligand. In 2017, Akogun and coworkers [19] designed and synthesized a reversible "turn-on" fluorescent sensor for selective detection of Zn^{2+}. In 2018, Hao et al. designed a reversible bis(salamo)-based fluorescence sensor for selective detection of Cd^{2+} in water-containing systems and food samples [23, 24]. In 2019, Dong et al. studied a highly sensitive and selective fluorescent "off-on-off" relay chemosensor based on a new bis(salamo)-type tetraoxime for detecting Zn^{2+} and CN^{-} [25]. Also, many Cu^{2+} and Zn^{2+} chemical sensors have been developed in the past few decades, and some Cu^{2+} and Zn^{2+} sensors have shown commercial application prospects. However, it is still necessary to design new sensors with better selectivity, stronger anti-interference ability, visual sensitivity, excellent reliability, easy synthesis, and low cost.

Continuing previous research work, a novel colorimetric and fluorescent sensor HL (HL = (E)-2-hydroxybenzaldehyde *O*-(2-(((E)-(4-(dimethylamino)benzylidene)amino)oxy)ethyl)oxime) for Cu^{2+} and Zn^{2+} ions was designed and synthesized. The structure of the HL sensor was confirmed by X-ray crystallography in addition to NMR and mass data. Such new HL sensor displays extreme selectivity for Cu^{2+} and Zn^{2+} in methanol solution compared to other metal ions examined. Signal transduction occurs via intramolecular charge transfer (ICT) and chelation-enhancement quenching (CHEQ) with Cu^{2+} and via chelation-enhanced fluorescence (CHEF) with Zn^{2+}. ^{1}H NMR, IR, and density functional theory (DFT) calculations are used to explain the mode of HL binding with metal ions.

Experimental. Fresh double-distilled water used throughout the experiments; 2-hydroxybenzaldehyde (98%) and p-dimethylaminobenzaldehyde (98%) were purchased from Alfa Aesar and used without further purification. Other reagents and solvents were analytical grade reagents from Tianjin Chemical Reagent Factory. Metal salts used were acetates of the general formula $M(CH_3COO)_n{\cdot}xH_2O$ except $Cr(NO_3)_3{\cdot}9H_2O$, $Al(NO_3)_3{\cdot}9H_2O$, $Pb(NO_3)_2$, and $HgCl_2$ in the experiments.

Melting points were measured on a Beijing Tektronix X-4 micro melting point apparatus. The elemental analysis for C, H, and N was performed using a GmbH VarioEL V3.00 automatic elemental analysis instrument; Cu and Zn analyses were performed using inductively coupled plasma absorption emission spectroscopy (ICP-AES), ^{1}HNMR spectra were obtained on a Mercury-400BB spectrometer. UV-Vis absorption spectra were measured on a U-3900H UV visible spectrophotometer. Fluorescence spectra were measured on an F-7000 FL spectrophotometer. Infrared (IR) spectra were obtained on a VERTEX-70 FT-IR spectrophotometer, with samples prepared as KBr (400–4000 cm^{-1}). All the spectra were recorded at room temperature.

Preparation of the HL sensor. The HL sensor was obtained by the synthetic route

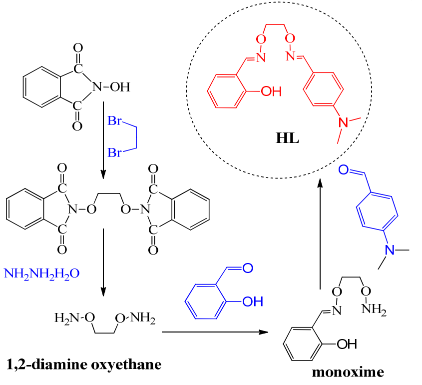

1,2-Diamine oxyethane and monoxime (2-[*O*-(1-ethyloxyamide)]oxime phenol) were prepared according to the methods reported earlier [26–32]. The HL sensor was synthesized via the Schiff base reactions [33, 34], in which 4-(*N*,*N*-dimethylamine) benzaldehyde (229.75 mg, 1.54 mmol) in ethanol (50 mL) was slowly dropped to a solution of 2-[*O*-(1-ethyloxyamide)]oxime-phenol (301.84 mg, 1.54 mmol) in ethanol (50 mL), and the mixture was stirred at 55°C for 24 h.

The reaction solution was distilled under reduced pressure, diluted with ethanol/hexane (8 mL, 1:4), and cooled in a refrigerator for 12 h to obtain a precipitate. Afterwards, the precipitate was purified by recrystallization with ethanol/hexane (1:4) and dried in vacuum to obtain a white powder HL. Yield: 75.5%, m.p. 74–75°C. Elemental analysis – calcd.: $C_{18}H_{21}N_3O_3$: C, 66.04%; H, 6.47%; N, 12.84%, O, 14.66%. Found: C, 66.03%; H, 6.48%; N, 12.83%. ^{1}H NMR (400 MHz, $CDCl_3$) δ 9.83 (s, 1H), 8.23 (s, 1H), 8.08 (s, 1H), 7.49 (d, *J* = 8.5 Hz, 2H), 7.31 – 7.24 (m, 1H), 7.15 (dd, *J* = 7.7, 1.7 Hz, 1H), 7.01 – 6.95 (m, 1H), 6.90 (dd, *J* = 7.5, 1.1 Hz, 1H), 6.85 (d, *J* = 3.1 Hz, 1H), 4.49 – 4.42 (m, 4H), 3.02 (s, 6H).

Results and discussion. *Colorimetric recognition of* Cu^{2+}. To obtain an insight into the selective recognition of the HL sensor toward metal ions, color changes of the HL solution (10 μM) to various metal ions (Cr^{3+}, Mn^{2+}, Fe^{2+}, Co^{2+}, Ni^{2+}, Cu^{2+}, Zn^{2+}, Cd^{2+}, Hg^{2+}, Al^{3+}, and Pb^{2+}) were investigated in the aqueous solution (CH_3OH/H_2O, 9:1, v/v, 10 mM). The single metal ion solution showed its intrinsic color. After adding the HL solution, compared with other metal ions, there is an obvious color change between HL and Cu^{2+} from blue to green that can be observed with the naked eye, which is obviously different from other metal ions. The above experiment results indicate that the HL sensor could be developed as a colorimetric sensor for Cu^{2+} ions.

UV-visible selective recognition for Cu^{2+}. To explore the selectivity of the HL sensor for common metal ions, a UV-visible selective recognition experiment was carried out (Fig. 1). It was found that Cu^{2+} caused a large change in the UV-visible absorption spectrum of the HL sensor. The red shift of the absorption spectrum indicated that the recognition moiety (-C=N-, -OH) linked to the electron-withdrawing group (-Ph-) of the HL sensor was coordinated with Cu^{2+} ions, which enhanced the electron withdrawing ability of the acceptor (Cu^{2+}) and the degree of conjugation of the L-Cu^{2+} system. It was preliminarily determined that the HL sensor had good UV-visible selectivity to Cu^{2+} ions, which could be explained by the recognition mechanism of intramolecular charge transfer (ICT) and ligand-to-metal charge transition (LMCT) [35–37].

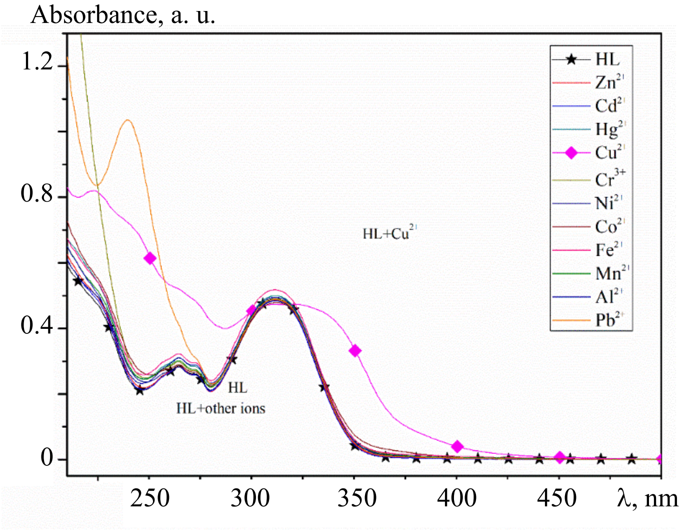

Fig. 1. UV-visible spectra of the HL sensor (10 μM) in the presence of 10 equiv. of various metal ions in $MeOH/H_2O$ solution.

UV-visible anti-interference recognition for Cu^{2+}. To test the single selective recognition ability of the HL sensor for Cu^{2+} in the multi-factor actual environment, L-Cu^{2+} anti-interference tests was carried out, and it was found that all potential competing metal cations had little or no effect on the selective recognition of the HL sensor for Cu^{2+}.

UV-visible sensitivity and reliability recognition for Cu^{2+}. In order to discuss the bonding properties of the HL sensor for Cu^{2+}, a titration experiment for the ultraviolet-visible absorption spectrum was carried out, as shown in Fig. 2. A methanol solution of Cu^{2+} (0–1.2 eq. 1 mM) was added dropwise to a methanol solution of the HL sensor (2 mL, 10 μM). The absorption spectrum of the HL sensor was gradually red-shifted (LMCT), and the absorption peaks (n–π*, π–π*) of the HL sensor at 310 (-C=N-O-) and 264 nm (-Ph-) were continuously weakened [26, 28]. A new absorption peak (-C=N-O-, π–π*, $\pi \rightarrow t_{2g}$) appeared at 320–420 nm, indicating that the oxime nitrogen atoms were coordinated with Cu^{2+}, and the absorption overlap line (-Pr-OH) at 255–275 nm was smaller, indicating that the coordination of phenolic oxygen atoms with Cu^{2+} had little effect on UV-visible absorption [29, 38, 39]. When the amount of Cu^{2+} added was close to or exceeds 1 equiv., the absorption spectrum changes little, which can preliminarily indicate that the HL sensor and Cu^{2+} were coordinated in a ratio of 1:1. Based on the absorbance at 350 nm, according to the Benesi–Hildebrand method, the equilibrium constant of the coordination reaction of the HL sensor and Cu^{2+} in a MeOH/H_2O solution was calculated to be 9.98×10^{13} M, and the correlation coefficient R^2 was 0.965. It can be seen that the complex formed by the HL sensors and Cu^{2+} is very stable. Taking the titration data point at 350 nm with $(A_{\min}-A)/(A_{\min}-A_{\max})$ as the ordinate and lg[Cu^{2+}] as the abscissa, the fitted line intersects the coordinate axis, and the detection limit of the HL sensor for Cu^{2+} in MeOH/H_2O solution was calculated to be 1.05×10^{-6} M.

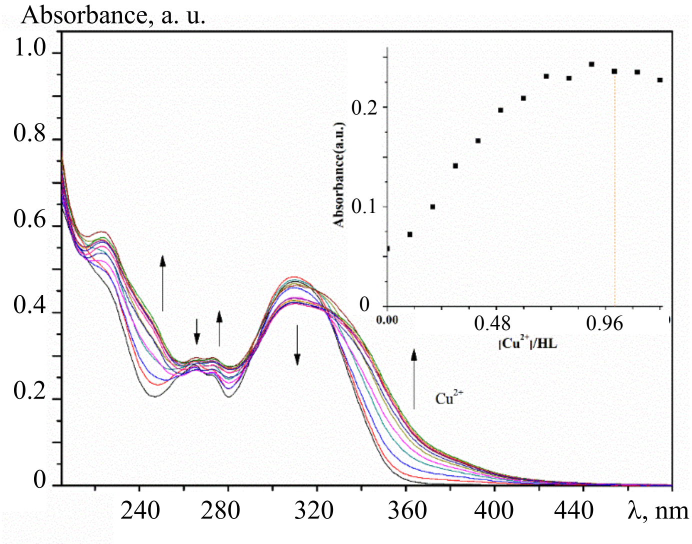

Fig. 2. Changes in the UV-Visible spectrum of the HL solution (10 μM) when adding different amounts of Cu^{2+} (0–1.0 equiv.).

Fluorescence selective recognition for Zn^{2+}. To explore the fluorescence selectivity of the HL sensor for common metal ions, a fluorescence selective recognition experiment was carried out (Fig. 3). It was found that the fluorescence emission spectrum of Zn^{2+} on the HL sensor was increased about two times, and the emission peak had a weak red shift (430.4→438.6 nm). However, Cd^{2+} had a weak influence on the fluorescence emission spectrum of the HL sensor, and the two lines mostly coincided. In contrast, the fluorescence emission spectrum of Cu^{2+} on the HL sensor was attenuated by about two times, and the emission peak was blue-shifted (430.4→408.8 nm) [32, 33]. Also, the fluorescence emission spectrum of Fe^{2+} on the HL sensor was reduced at least twice, and the emission peak was blue-shifted (430.4→407 nm). Other metal ions have different degrees of attenuation and blue shifting in the fluorescence emission spectrum of the HL sensor. These phenomena indicated that charge transfer (LMCT) might occur in the L-Zn^{2+} complex. It was preliminarily concluded that the HL sensor can be used for fluorescence selective recognition of Zn^{2+} and Cu^{2+} as a chelation-enhanced fluorescence effect (CHEF) sensor for Zn^{2+} ions, and as a chelation-enhancement quenching effect sensor (CHEQ) for Cu^{2+} [18, 19].

Fluorescence anti-interference recognition for Zn^{2+}. In order to explore the selective recognition of the HL sensor for Zn^{2+} in the presence of other metal ions, interference tests were conducted in the presence of Zn^{2+} (excess amounts). When the HL sensor was treated with 5.0 equiv. of Zn^{2+} in the presence of excess amounts (5.0 equiv.) of other metal ions, the coexisting metal ions had little or negligible effect on the emission response of the HL sensor for Zn^{2+}, except for the anticipated quenching effect produced by Cu^{2+}, Fe^{2+}, Co^{2+}, and Ni^{2+}, which might be due to their paramagnetic nature. This suggested that further study of the HL sensor could make it suitable for detecting Cu^{2+} in the opposite direction due to its quenching ability. Moreover, Cd^{2+} did not inhibit the emission intensity of Zn^{2+}. These results show that the HL sensor can well distinguish between Zn^{2+} and Cd^{2+}, which usually have similar properties, and other cations with opposite directions that used as a fluorescence anti-interference sensor for identifying Zn^{2+} [18, 19, 40].

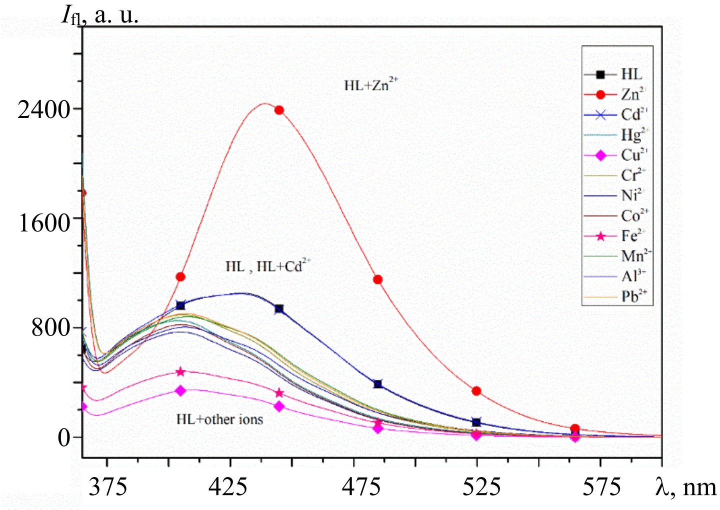

Fig. 3. Fluorescence emission spectra of the HL sensor (10 μM) in the presence of 10 equiv. of various metal ions in $MeOH/H_2O$ solution ($MeOH/H_2O$ = 9:1, *v/v*). (EX WL: 350.0 nm, EX Slit: 10.0 nm, EM Slit: 20.0 nm, PMT Voltage: 400 V).

Fluorescence sensitivity and reliability recognition for Zn^{2+}. Subsequently, the binding affinity of the HL sensor with Zn^{2+} was examined through a fluorescence titration experiment, in which different concentrations of Zn^{2+} were added to the HL sensor solution (10 μM). The emission intensity at 444 nm was gradually increased. The fluorescence changes terminated when 1 equiv of Zn^{2+} was employed (Fig. 4). Moreover, the linear relationships of the HL sensor toward Zn^{2+} in low concentration ranges showed that a reasonable linear relationship could be built when the concentration of Zn^{2+} did not exceed 1 equiv. of the HL sensor. The constant K of the HL sensor binding to Zn^{2+} was estimated to be 7.09×10^{11} M by the Benesi–Hildebrand equation (fluorescence method) [41]. Moreover, the detection limit of the HL sensor for Zn^{2+} was evaluated to be 2.84×10^{-7} M [42].

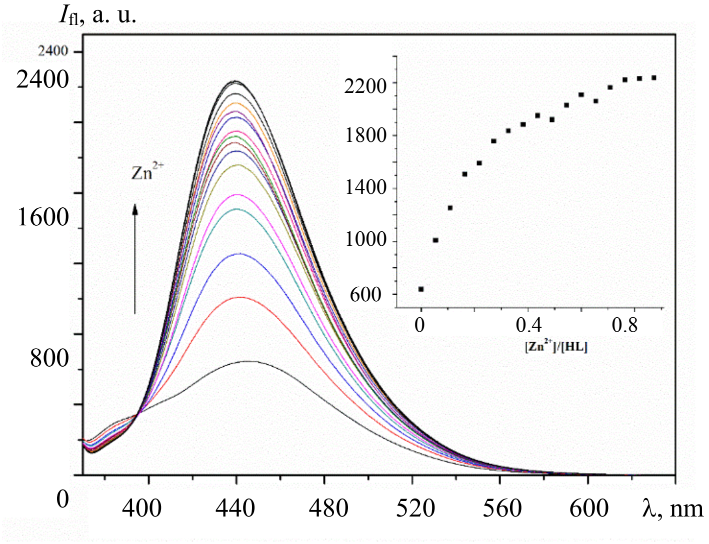

Fig. 4. Changes in the fluorescence spectrum of the HL solution (10 μM) upon addition of different amounts of Zn^{2+} (0–1.0 equiv.). (EX WL: 350.0 nm, EX slit: 10.0 nm, EM slit: 20.0 nm, PMT voltage: 400 V).

Compared with the titration results of UV-visible spectroscopy of the HL sensor by Cu^{2+}, it can be seen that the complex formed by the HL sensor for Zn^{2+} is less stable than the complex reacted from the HL sensor for Cu^{2+}, so Zn^{2+} in the L-Zn^{2+} complex can be replaced by Cu^{2+}. From $\Delta G^{\theta} = -RT\ln K^{\theta}$, the energy changes of the coordination reaction of the HL sensor for Cu^{2+} and for Zn^{2+} at the standard temperature (273.15 K) can be calculated as –7.32 and –6.2 KJ/mol, respectively.

The recognition mechanism of the HL sensor for Cu^{2+} and Zn^{2+} by IR spectra inspection. The recognition mechanism of the HL sensor for Cu^{2+} and Zn^{2+} was inspected by IR spectra (Fig. 5). The band at 3419 cm^{-1} (HL), which corresponds to the characteristic phenolic hydroxyl absorption, was shifted to 3430 cm^{-1} when combining Zn^{2+}, and 3466 cm^{-1} when combining Cu^{2+}, indicating the presence of a multi-molecule association and molecular hydrogen bonds in the complexes [26, 28, 43, 44]. The band at 1611 cm^{-1} (HL), which corresponds to the characteristic C=N absorption, was shifted to 1610 cm^{-1} when combining Zn^{2+}, and 1607 cm^{-1} when combining Cu^{2+} [29, 32, 45]. The band at 1257 cm^{-1} (HL), attributed to the stretching vibration band $\nu_{Ar–O}$ of the phenolic group, appeared in the low wavenumber direction in both complexes [33, 46]. These results supported that a strong binding participation occurs between the phenolic group, C=N group, and the metal ions (Cu^{2+} and Zn^{2+}) [47–49].

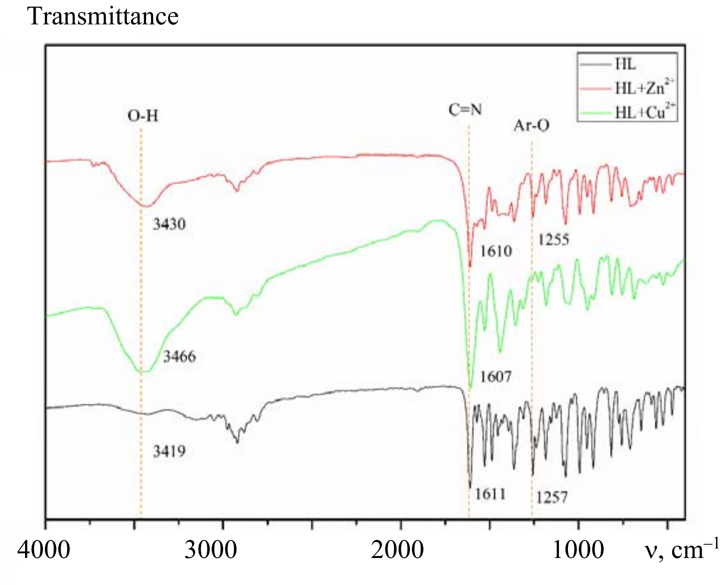

Fig. 5. IR spectra of the HL sensor, L-Cu^{2+} complex, and L-Zn^{2+} complex in KBr disks.

The recognition mechanism of sensor HL for Cu^{2+} and Zn^{2+} by ^1H NMR. The mechanism of interaction between the HL sensor and Cu^{2+} was further studied by investigation of the ^1H NMR of the complex (L-Cu^{2+}), as shown in Fig. 6.

The HL sensor in $CDCl_3$ solution was in full contact with the solution of $Cu(OAc)_2{\cdot}H_2O$ in D_2O, and the organic phase was extracted and separated for ^1H NMR spectroscopy analysis. The new peak appearing at 2.62 ppm of chemical shift was assigned to methyl hydrogen ($–CH_3$) of acetate, and the integration results indicated that there should be two molecules of acetate in the complex molecule (L-Cu^{2+}). The disappearance of the proton peak at 9.83 ppm (–OH) indicated dehydrogenation of the phenolic hydroxyl group and coordination with Cu^{2+}, and the electrons were transferred from the electron-rich O to the empty *d* orbital of Cu^{2+}. The proton peak at 8.23 ppm (-N=CH-) remained unchanged, and the proton peak at 8.08 ppm (-HC=N-) shifted to the high field (8.06 ppm), suggesting that the electron transferred from metal ions Cu^{2+} to the HL sensor molecules (LMCT). At the same time, the coordination between N atoms of -HC=N- (8.08 ppm) and Cu^{2+} might occur, and the increase of electron cloud density on -HC=N-group might further enhance the PET process of the sensor, resulting in fluorescence quenching. The ^1H NMR of the L-Zn^{2+} complex, the same as that of the HL sensor, may mean poor stability of the outer rail type L-Zn^{2+} complex, in sharp contrast to the inner rail L-Cu^{2+} complex [50–52].

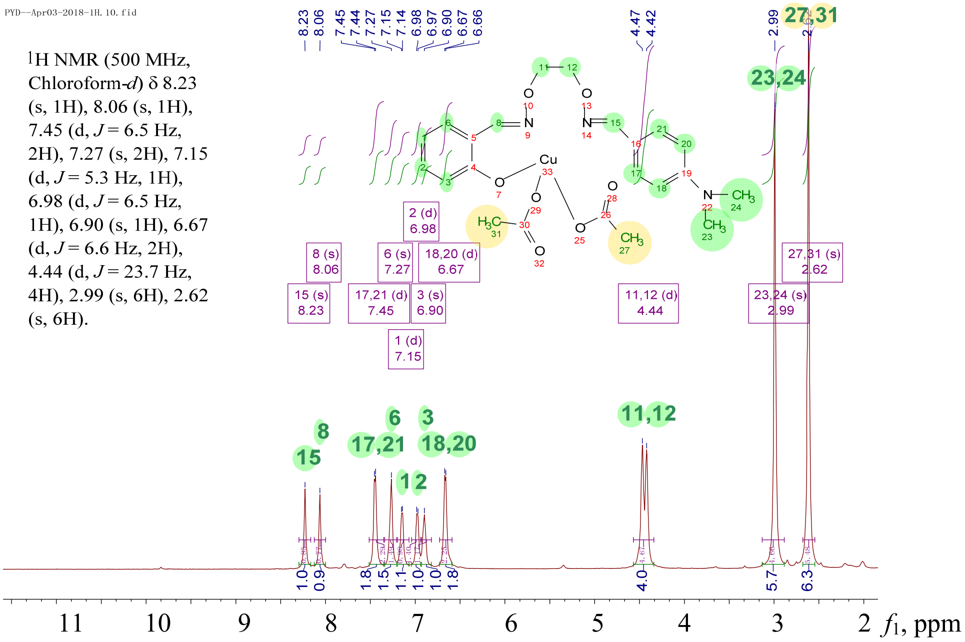

^{1}H NMR (500 MHz, Chloroform-*d*) δ 8.23 (s, 1H), 8.06 (s, 1H), 7.45 (d, *J* = 6.5 Hz, 2H), 7.27 (s, 2H), 7.15 (d, *J* = 5.3 Hz, 1H), 6.98 (d, *J* = 6.5 Hz, 1H), 6.90 (s, 1H), 6.67 (d, *J* = 6.6 Hz, 2H), 4.44 (d, *J* = 23.7 Hz, 4H), 2.99 (s, 6H), 2.62 (s, 6H).

Fig. 6. Identification mechanism of the probe HL molecule for Cu^{2+}.

DFT optimization of the HL sensor, L-Cu^{2+} and L-Zn^{2+} complexes. To study the recognition mechanism and coordination configuration of the L-$Cu^{2+}$and L-Zn^{2+} complexes, the geometries of the HL sensor, L-Cu^{2+} and L-Zn^{2+} complexes were simulated according to the relevant literature [53, 54] and optimized using the Gaussian 09 package at B3LYP/6-31G(*d*) levels for C, H, O, N atoms and LANL2DZ levels for Cu^{2+} and Zn^{2+}. The minimum natures of the structures were confirmed by frequency calculations at the same computational level [55, 56]. The calculation results are shown in Fig. 7. The central ion Cu^{2+} ($t_{2g}^6e_g^3$) of the L-Cu^{2+} complex might adopt the planar tetragonal configuration (D_{4h}) of the deformed octahedron with dsp^2 hybri-

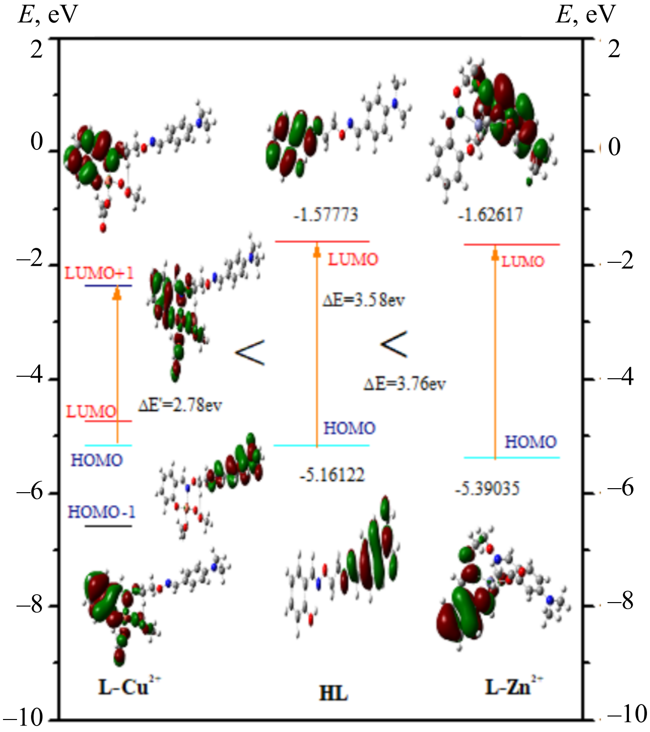

Fig. 7. Surface plots of HOMO, LUMO of the HL sensor (middle), L-Cu^{2+} complex (left) and the L-Zn^{2+} complex (right).

dization, and the central ion Zn^{2+} (d^{10}) of L-Zn^{2+} complex might take the distorted octahedral triangular bipyramidal configuration (D_{3h}) by sp^3d hybridization. The ΔE value of the HL sensor, $\Delta E = E_{\mathrm{LUMO}} - E_{\mathrm{HOMO}} =$ $= 3.58$ eV ($\lambda_{\mathrm{edge}} = 370$ nm), could be consistent with the results obtained by UV-visible absorption spectroscopy ($E_g^{\mathrm{opt}} = 3.35$ eV). The band gap value might become smaller after coordination with Cu^{2+} [$\Delta E' =$ $= E_{\mathrm{LUMO+1}} - E_{\mathrm{HOMO}} = (-2.35244) - (-5.13265) = 2.78$ eV ($\lambda_{\mathrm{edge}} = 446$ nm)], and larger after coordination with Zn^{2+} ($\Delta E = E_{\mathrm{LUMO}} - E_{\mathrm{HOMO}} = 3.76$ eV). According to the frontier orbital theory, the HOMO energy of the L-Cu^{2+} complex could be between the LUMO and HOMO energy of the HL sensor. When the recognition group of the HL sensor is combined with Cu^{2+} ion, the electron donation ability is enhanced and the oxidation potential is reduced. The orbital energy level may be higher than the corresponding orbital energy level of the fluorophore, resulting in enhancement of the PET process. At this time, the electrons excited by photons in the fluorophore cannot directly jump back to the original ground state orbit, resulting in fluorescence quenching. On the other hand, the HOMO energy level of the L-Zn^{2+} complex could be lower than that of the HL sensor. When the recognition group binds to the Zn^{2+} ion, the oxidation potential of the recognition group might increase and the electron donating ability may decrease due to the presence of LMCT; the electron donating ability will decrease, resulting in the orbital energy level being lower than the corresponding level of the fluorophore orbital energy. In addition, since the PET process is blocked, photostimulated electrons in the fluorescent group could directly transfer back to the original ground state orbit channel, resulting in enhanced fluorescence.

Conclusions. A novel tridentate bisoxime HL sensor with phenolic hydroxyl and oxime ether as recognition group for Cu^{2+} and Zn^{2+} was designed and synthesized. The HL sensor displayed an extreme colorimetric (blue becomes grass green) and UV visible selectivity for Cu^{2+} recognition, as well as good fluorescence selectivity for Zn^{2+} (fluorescence on) and Cu^{2+} (fluorescence off) compared to other metal ions examined in CH_3OH/H_2O solution. The UV-visible spectroscopy analyses show that the coordination ratio of the HL sensor to Cu^{2+} is 1:1 with a large binding constant (9.98×10^{13} M) and a minimum detection limit (1.05×10^{-6} M) in CH_3OH/H_2O solution. The fluorescence spectroscopy analyses reveal that the coordination ratio of the HL sensor to Zn^{2+} is 1:1 with a moderate binding constant (7.09×10^{11} M), and a minimum detection limit (2.84×10^{-7} M) in CH_3OH/H_2O solution. The nuclear magnetic titration experiment and DFT calculations indicate that the fluorescence quenching recognition mechanism of the HL sensor for Cu^{2+} may be enhanced by the PET process, and the fluorescence enhancement recognition mechanism of the HL sensor to Zn^{2+} may be hindered by the PET process. Variations in the ligands on the aromatic group (Ar-CH=NO-$(CH_2)_2$-ON=CH-Ar') may provide the possibility for the selective recognition of different metal ions.

Acknowledgements. This work was supported by Youth Science Foundation of Gansu Province (20JR5RF611), the National Natural Science Foundation of China (21761018) and the Program for Excellent Team of Scientific Research in Lanzhou Jiaotong University (201706), three of which are gratefully acknowledged.

REFERENCES

1. J. Y. Kwon, Y. J. Jang, Y. J. Lee, K. M. Kim, M. S. Seo, W. Nam, J. Yoon, *J. Am. Chem. Soc.*, **127**, 10107–10111 (2005).
2. S. K. Kim, N. J. Singh, S. J. Kim, H. G. Kim, J. K. Kim, J. W. Lee, K. S. Kim, J. Yoon, *Org. Lett.*, **5**, 2083–2086 (2003).
3. L. Wang, Z. L. Wei, Z. Z. Chen, C. Liu, W. K. Dong, Y. J. Ding, *Microchem. J.*, **155**, 104801 (2020).
4. K. B. Kim, D. M. You, J. H. Jeon, Y. H. Yeon, J. H. Kim, C. Kim, *Tetrahedron Lett.*, **55**, 1347–1352 (2014).
5. C. Liu, Z. L. Wei, H. R. Mu, W. K. Dong, Y. J. Ding, *J. Photochem. Photobiol. A*, **397**, 112569 (2020).
6. L. Wang, Z. L. Wei, C. Liu, W. K. Dong, J. X. Ru, *Spectrochim. Acta A*, **239**, 118496 (2020).
7. H. R. Mu, M. Yu, L. Wang, Y. Zhang, Y. J. Ding, *Phosphorus Sulfur Silicon Relat. Elem.,* **195**, 730–739 (2020).
8. L. Wang, Y. Q. Pan, J. F. Wang, Y. Zhang, Y. J. Ding, *J. Photochem. Photobiol. A*, **400**, 112719 (2020).
9. R. N. Bian, J. F. Wang, Y. J. Li, Y. Zhang, W. K. Dong, *J. Photochem. Photobiol. A*, **403**, 112829 (2020).
10. X. Xu, R. N. Bian, S. Z. Guo, W. K. Dong, Y. J. Ding, *Inorg. Chim. Acta*, **513**, 119945 (2020).
11. Y. D. Peng, Y. Zhang, Y. L. Jiang, Z. L. Ren, F. Wang, L. Wang, *J. Fluoresc.*, **30**, 1049 (2020).
12. M. D. Tutulea-Anastasiu, D. Wilson, M. del Valle, *Sensors*, **13**, 4367–4377 (2013).

13. L. Hu, H. Wang, B. Fang, Z. Y. Hu, Q. Zhang, X. H. Tian, H. P. Zhou, J. Y. Wu, Y. P. Tian, *Sens. Actuat. B*, 251 (2017).
14. F. U. Rahman, S. B. Yu, S. K. Khalil, Y. P. Wu, S. Koppireddi, Z. T. Li, H. Wang, D. W. Zhang *Sens. Actuat. B*, **263**, 594–604 (2018).
15. T. Jia, M. Fu, M. Y. Zhang, J. W. Qiu, H. Zhu, Y. Gao, *Spectrochim. Acta A*, 1386–1425 (2019).
16. H. G. Classen, U. Gröber, D. Löw, J. Schmidt, H. Stracke, *Med. Monatsschr. Pharm.*, **34**, 87–95 (2011).
17. P. Wang, J. Wu, *Spectrochim. Acta A*, **208**, 140–149 (2019).
18. Z. L. Wei, L. Wang, S. Z. Guo, Y. Zhang, W. K. Dong, *RSC Adv.*, **9**, 41298–41303 (2019).
19. L. Z. Liu, L. Wang, M. Yu, Q. Zhao, Y. Zhang, Y. X. Sun, W. K. Dong, *Spectrochim. Acta A,* **222**, 117209 (2019).
20. H. Irving, R. J. P. Williams, *J. Chem. Soc.*, 3192–3210 (1953).
21. N. Chitrapriya, V. Mahalingam, L. C. Channels, M. Zeller, F. R. Fronczek, K. Natarajan, *Inorg. Chim. Acta*, **361**, 2841–2850 (2008).
22. N. Mergu, V. K. Gupta, *Sens. Actuat. B*, **210**, 408–417 (2015).
23. F. Wang, L. Z. Liu, L. Gao, W. K. Dong, *Spectrochim. Acta A*, **203**, 56–64 (2018).
24. J. Hao, X. Y. Li, Y. Zhang, W. K. Dong, *Materials*, **11**, 523 (2018).
25. L. Z. Liu, L. Wang, M. Yu, Q. Zhao, Y. Zhang, Y. X. Sun, W. K. Dong, *Spectrochim. Acta A*, **222**, 117209 (2019).
26. L. Wang, Z. L. Wei, M. Yu, Y. Q. Pan, Y. Zhang, W. K. Dong, *Chin. J. Inorg. Chem.*, **35**, 1791–1804 (2019).
27. Y. Zhang, M. Yu, Y. Q. Pan, Y. Zhang, L. Xu, W. K. Dong, *Appl. Organomet. Chem.,* **34**, e5442 (2020).
28. Y. F. Cui, Y. Zhang, K. F. Xie, W. K. Dong, *Crystals*, **9**, 596 (2019).
29. Y. Zhang, Y. Q. Pan, M. Yu, X. Xu, W. K. Dong, *Appl. Organomet. Chem.*, **33**, e5240 (2019).
30. Z. L. Ren, J. Hao, P. Hao, X. Y. Dong, Y. Bai, W. K. Dong, *Z. Naturforsch.*, **73b**, 203–210 (2018).
31. Q. P. Kang, X. Y. Li, L. Wang, Y. Zhang, W. K. Dong, *Appl. Organomet. Chem.,* **33**, e5013 (2019).
32. X. X. An, C. Liu, Z. Z. Chen, K. F. Xie, W. K. Dong, *Crystals*, **9**, 602 (2019).
33. L. Xu, M. Yu, L. H. Li, J. C. Ma, W. K. Dong, *J. Struct. Chem.*, **60**, 1358–1365 (2019).
34. Q. P. Kang, X. Y. Li, Z. L. Wei, Y. Zhang, W. K. Dong, *Polyhedron*, **165**, 38–50 (2019).
35. M. Yu, H. R. Mu, L. Z. Liu, N. Li, Y. Bai, X. Y. Dong, *Chin. J. Inorg. Chem.,* **35**, 1109–1120 (2019).
36. X. X. An, Z. Z. Chen, H. R. Mu, L. Zhao, *Inorg. Chim. Acta*, **511**, 119823 (2020).
37. X. X. An, Q. Zhao, H. R. Mu, W. K. Dong, *Crystals*, **9**, 101 (2019).
38. Y. Q. Pan, X. Xu, Y. Zhang, Y. Zhang, W. K. Dong, *Spectrochim. Acta A*, **229**, 117929 (2020).
39. M. Yu, Y. Zhang, Y. Q. Pan, L. Wang, *Inorg. Chim. Acta*, **509**, 119701 (2020).
40. H. A. Benesi, J. H. Hildebrand, *J. Am. Chem. Soc.*, **71**, 2703–2707 (1949).
41. H. H. Wang, L. Xue, H. Jiang, *Org. Lett.*, **13**, 3844–3847 (2011).
42. Y. X. Sun, Y. Q. Pan, X. Xu, Y. Zhang, *Crystals*, **9**, 607 (2019).
43. Y.Q. Pan, Y. Zhang, M. Yu, Y. Zhang, L. Wang, *Appl. Organomet. Chem.,* 34, e5441 (2020).
44. H. R. Mu, X. X. An, C. Liu, Y. Zhang, W. K. Dong, *J. Struct. Chem.*, **61**, 1155–1166 (2020).
45. S. Z. Zhang, J. Chang, H. J. Zhang, Y. X. Sun, Y. Wu, Y. B. Wang, *Chin. J. Inorg. Chem.*, **36**, 503–514 (2020).
46. Y. Zhang, Y. J. Li, S. Z. Guo, T. Fu, L. Zhao, *Transit. Met. Chem.*, **45**, 485–492 (2020).
47. L. W. Zhang, Y. Zhang, Y. F. Cui, M. Yu, W. K. Dong, *Inorg. Chim. Acta*, **506**, 119534 (2020).
48. Q. Zhao, X. X. An, L. Z. Liu, W. K. Dong, *Inorg. Chim. Acta*, **490**, 6–15 (2019).
49. L. Z. Liu, M. Yu, X.Y. Li, Q. P. Kang, W. K. Dong, *Chin. J. Inorg. Chem.*, **35**, 1283–1294 (2019).
50. Y. Zhang, L. Z. Liu, Y. D. Peng, N. Li, W. K. Dong, *Transit. Met. Chem.*, **44**, 627–639 (2019).
51. X. Y. Li, Q. P. Kang, C. Liu, Y. Zhang, W. K. Dong, *New J. Chem.*, **43**, 4605–4619 (2019).
52. Z. L. Wei, L. Wang, J. F. Wang, W. T. Guo, Y. Zhang, W. K. Dong, *Spectrochim. Acta A*, **229**, 117775 (2020).
53. C. Liu, X. X. An, Y. F. Cui, K. F. Xie, W. K. Dong, *Appl. Organomet. Chem.*, **34**, e5272 (2020).
54. J. Chang, S. Z. Zhang, Y. Wu, H. J. Zhang, Y. X. Sun, *Transit. Met. Chem.*, **45**, 279–293 (2020).
55. M. J. Frisch, G. W. Trucks, H. B. Schlegel, G. E. Gaussian 09, Revision B. 01, Gaussian, Inc., Wallingford CT, Wallingford CT (2009).
56. B. Kosar, C. Albayrak, *Spectrochim. Acta A*, **78**, 160–167 (2011).